THE JOURNAL OF BIOLOGICAL CHEMISTRY VOL. 288, NO. 49, pp. 35534–35547, December 6, 2013
© 2013 by The American Society for Biochemistry and Molecular Biology, Inc. Published in the U.S.A.

Protein Arginine Methyltransferase 5 (PRMT5) Inhibition Induces Lymphoma Cell Death through Reactivation of the Retinoblastoma Tumor Suppressor Pathway and Polycomb Repressor Complex 2 (PRC2) Silencing*

Received for publication, August 14, 2013, and in revised form, November 1, 2013 Published, JBC Papers in Press, November 4, 2013, DOI 10.1074/jbc.M113.510669

Jihyun Chung[‡], Vrajesh Karkhanis[‡], Sookil Tae[‡], Fengting Yan[§], Porsha Smith[§], Leona W. Ayers[¶], Claudio Agostinelli[‖], Stefano Pileri[‖], Gerald V. Denis[**], Robert A. Baiocchi[§], and Saïd Sif[‡1]

*From the Departments [‡]Molecular and Cellular Biochemistry and [¶]Pathology and [§]Division of Hematology, College of Medicine, The Ohio State University, Columbus, Ohio 43210, the [‖]Hematopathology Unit, Department of Experimental, Diagnostic and Specialty Medicine (DIMES), University of Bologna, 40126 Bologna, Italy, and the **Cancer Research Center, Boston University School of Medicine, Boston, Massachusetts 02118*

Background: PRMT5, PRC2, and cyclin D1 are overexpressed in non-Hodgkin lymphoma (NHL).
Results: PRMT5 expression inversely correlates with levels of hypophospho-RB1 and RBL2.
Conclusion: PRMT5 inhibition reactivates RB1 and RBL2 and silences PRC2 and cyclin D1.
Significance: PRMT5 inhibition results in NHL growth arrest and cell death.

Epigenetic regulation mediated by lysine- and arginine-specific enzymes plays an essential role in tumorigenesis, and enhanced expression of the type II protein arginine methyltransferase PRMT5 as well as the polycomb repressor complex PRC2 has been associated with increased cell proliferation and survival. Here, we show that PRMT5 is overexpressed in three different types of non-Hodgkin lymphoma cell lines and clinical samples as well as in mouse primary lymphoma cells and that it up-regulates PRC2 expression through inactivation of the retinoblastoma proteins RB1 and RBL2. Although PRMT5 epigenetically controls RBL2 expression, it indirectly promotes RB1 phosphorylation through enhanced cyclin D1 expression. Furthermore, we demonstrate that PRMT5 knockdown in non-Hodgkin lymphoma cell lines and mouse primary lymphoma cells leads to RBL2 derepression and RB1 reactivation, which in turn inhibit PRC2 expression and trigger derepression of its *CASP10*, *DAP1*, *HOXA5*, and *HRK* pro-apoptotic target genes. We also show that reduced PRMT5 expression leads to cyclin D1 transcriptional repression via loss of TP53K372 methylation, which results in decreased BCL3 expression and enhanced recruitment of NF-κB p52-HDAC1 repressor complexes to the cyclin D1 promoter. These findings indicate that PRMT5 is a master epigenetic regulator that governs expression of its own target genes and those regulated by PRC2 and that its inhibition could offer a promising therapeutic strategy for lymphoma patients.

During B cell development, several DNA recombination and modification events take place so that proper populations of pre-B cells are formed (1, 2). However, as B cells differentiate, aberrant DNA mutations and translocation may occur and lead to B cell transformation (3). Examples of B cell tumors at this stage of B cell development include mantle cell lymphoma (MCL),[2] which represents 3–10% of non-Hodgkin lymphoma (NHL) derived from a subset of naïve pre-germinal center (GC) B cells located in primary lymphoid follicles or in the mantle region of secondary lymphoid follicles. The hallmark of this disease is the translocation t(11;14)(q13;q32), which is detected in most if not all of cases and which juxtaposes the cyclin D1 gene at 11q13 to the immunoglobulin heavy chain locus at 14q32 (4). MCL is considered incurable, and affected patients often have a short median survival, highlighting the need for new therapeutic strategies (5, 6).

Upon encountering antigen, naïve B cells are activated and undergo GC reaction before they become mature B cells. During the GC reaction, B cells may transform into either follicular lymphoma or GC B cell-like diffuse large B cell lymphoma (GCB-DLBCL), and even after maturation, B cells remain susceptible to transformation, as shown in the case of activated B cell-like DLBCL (ABC-DLBCL) (2, 3). DLBCL is the most common NHL worldwide and has been divided by global gene expression profiling into three different types: GCB-DLBCL, ABC-DLBCL, and primary mediastinal B cell lymphoma (7, 8). Although most GCB-DLBCL patients can be cured with the anti-CD20 antibody rituximab combined with chemotherapy, >50% of ABC-DLBCL patients do not survive. Despite molecular profiling of MCL, GCB-DLBCL, and ABC-DLBCL, we still do not understand the molecular mechanisms that drive their initiation, maintenance, and progression.

* This work was supported, in whole or in part, by National Institutes of Health Grant R01 CA116093 from NCI (to S. S.). This work was also supported by the Leukemia Research Foundation MCL Initiative and Associazione Italiana per la Ricerca sul Cancro (AIRC) 5X100 Grant 10007 (to S. P.).
[1] To whom correspondence should be addressed. Tel.: 614-247-7445; Fax: 614-292-4118; E-mail: sif.1@osu.edu.

[2] The abbreviations used are: MCL, mantle cell lymphoma; NHL, non-Hodgkin lymphoma; GC, pre-germinal center; GCB-DLBCL, GC B cell-like diffuse large B cell lymphoma; ABC-DLBCL, activated B cell-like DLBCL; sh-GFP, GFP shRNA; RIPA, radioimmune precipitation assay; TMA, tissue microarray; TRITC, tetramethylrhodamine isothiocyanate.

It is well established that altered expression of oncogenes and/or tumor suppressor genes results in transformation of normal cells into malignant derivatives (9). Both activation and repression of target genes with growth regulatory functions have been reported in every cancer examined, and the mechanisms that lead to their dysregulation almost invariably involve epigenetic modification of chromatin (9–11). Although DNA methylation has clearly been implicated in gene silencing and tumorigenesis, methylation of histones at conserved lysine and arginine residues has also been shown to play an important role in cancer (12). Hypermethylation of histones H3R8 and H4R3 by the protein arginine methyltransferase PRMT5 has been documented in many cancers and shown to be associated with tumor cell growth and survival (13, 14). Similarly, increased levels of EZH2 (enhancer of zeste homolog 2), the catalytic subunit of the polycomb repressor complex PRC2, and its associated H3(Me_3)K27 mark have been reported in both solid and lymphoid tumors (15, 16).

PRMT5 is a member of the protein arginine methyltransferase family of enzymes that can symmetrically methylate arginine residues in a variety of cellular proteins, including histones (13). A consequence of PRMT5-induced histones H3R8 and H4R3 is transcriptional repression of target tumor suppressor genes (17–19). PRC2 consists of four core subunits, EZH2, SUZ12 (suppressor of zeste 12 homolog), EED (embryonic ectoderm development), and RBBP4/7 (retinoblastoma binding protein 4/7), and is involved in transcriptional silencing of growth and developmentally regulated genes (20, 21). Previous work has shown that expression of EZH2 and EED is controlled by E2F transcription factors, which are known to be modulated by the retinoblastoma family of tumor suppressors (22, 23). More recently, work by our group has demonstrated that PRMT5 epigenetically silences *RBL2,* which can in turn potentiate E2F function and promote cell proliferation (18). Given these results and the fact that expression of PRMT5 and PRC2 is enhanced in a variety of cancer cells, we reasoned that through its ability to suppress RBL2 expression, PRMT5 might positively control PRC2 levels.

Using patient-derived cell lines from three different NHL cell types, we show that PRMT5 promotes PRC2 expression through transcriptional silencing of *RBL2* and hyperphosphorylation of RB1. We also show that inhibition of PRMT5 by shRNA-mediated knockdown reactivates both RB1 and RBL2 tumor suppressors; restores recruitment of repressor complexes to the promoter regions of *EZH2*, *SUZ12*, and *EED*; and re-establishes expression of PRC2 pro-apoptotic target genes *CASP10*, *DAP1* (death-associated protein 1), *HOXA5*, and *HRK* (*Harakiri*). The net outcome of these molecular changes is inhibition of NHL cell growth and induced cell death. Furthermore, we show that the levels of PRMT5, PRC2, and their epigenetic marks are elevated in MCL, GCB-DLBCL, and ABC-DLBCL human clinical samples and that both RB1 and RBL2 are inactivated in NHL patient samples. To substantiate our findings, we show that PRMT5 and PRC2 levels are elevated in mouse primary lymphoma cells and that PRMT5 knockdown re-establishes RB1/RBL2-E2F regulation, which in turn reduces PRC2 levels and derepresses *DAP1*, *HOXA5*, and *HRK* target genes. Taken together, these findings demonstrate the role played by PRMT5 in the control of NHL cell growth and survival.

EXPERIMENTAL PROCEDURES

Plasmid Construction and Cell Infection—PRMT5 knockdown was achieved using lentiviral constructs that express two *PRMT5*-specific shRNAs (sh-PRMT5-1 and sh-PRMT5-2) as described previously (24). Briefly, plasmids pLenti×2DEST/sh-PRMT5-1, pLenti-CMV-GFP-DEST/sh-PRMT5-1, and pLenti×2DEST/sh-PRMT5-2 were constructed by first cloning double-stranded oligonucleotides that encode *PRMT5*-specific shRNAs into the entry vector pENTER/pTER$^+$. Plasmids pLenti×2DEST/sh-PRMT5-1 and pLenti-CMV-GFP-DEST/sh-PRMT5-1 were constructed using sense-1 (5′-GATCCCGCCCAGTTTGAGATGCCTTATGTGTGCTGTCCATAAGGCATCTCAAACTGGGCTTTTTGGAAA-3′) and antisense-1 (5′-AGCTTTTCCAAAAAGCCCAGTTTGAGATGCCTTATGGACAGCACACATAAGGCATCTCAAACTGGGCGG-3′) primers, whereas plasmid pLenti×2DEST/sh-PRMT5-2 was constructed using sense-2 (5′-AAAAACACTTCATATGTCTGAGACCTGTCTC-3′) and antisense-2 (5′-AATCTCAGACATATGAAGTGTTTCCTGTCTC-3′) primers, both of which were designed to include sticky ends compatible with BglII and HindIII and were cloned into the BglII- and HindIII-linearized pENTER/pTER$^+$ vector. Positive clones were identified by EcoRI digestion and confirmed by DNA sequencing. Next, plasmids pENTER/pTER$^+$/sh-PRMT5-1 and pENTER/pTER$^+$/sh-PRMT5-2 were individually recombined into either the pLenti×2DEST or pLenti-CMV-GFP-DEST vector as described previously (24), and positive clones were identified by EcoRV digestion in the case of pLenti×2DEST/sh-PRMT5-1 and pLenti×2DEST/sh-PRMT5-2 or by EcoRI digestion in the case of pLenti-CMV-GFP-DEST/sh-PRMT5-1, followed by DNA sequencing. To generate lentiviral particles that express *PRMT5*-specific shRNA, plasmid pLenti×2DEST/sh-PRMT5-1, pLenti×2DEST/sh-PRMT5-2, or pLenti-CMV-GFP-DEST/sh-PRMT5-1 was transfected along with pLP1, pLP2, and pVSG into 293T cells, and 72 h later, the supernatant was harvested and used to infect NHL or Eμ-BRD2 lymphoma cells as described previously (25).

Cell Culture, B Cell Isolation, and FACS Analysis—NHL cell lines and mouse primary Eμ-BRD2 lymphoma cells were grown in RPMI 1640 medium supplemented with 10% FBS and 1 mM sodium pyruvate. Normal human B cells were collected under an institutional review board-approved and Health Insurance Portability and Accountability Act-compliant protocol and isolated from tonsilar tissues as described previously (17). Mouse normal B cells were isolated from spleens of FVB mice using CD19 MicroBeads (Miltenyi Biotec) as specified by the manufacturer, whereas mouse primary Eμ-BRD2 lymphoma cells were purified from spleens of FVB female mice (Taconic Farms, Germantown, NY) that were sublethally irradiated with 4 grays using an RS-2000 irradiator and maintained on water containing sulfamethoxazole (0.8 mg/ml) and trimethoprim (0.16 mg/ml) as described previously (26). To evaluate proliferation of lymphoma cells, an equal number (8×10^5) of parental cells infected with lentivirus expressing either control GFP shRNA (sh-GFP) or sh-PRMT5-1 were plated in 6-well plates, and viable cells were counted every 2 days for 6 days using trypan blue

dye exclusion. To assess the effect of PRMT5 inhibition on cell death, 8×10^5 control sh-GFP or test sh-PRMT5-1 cells were seeded into 6-well plates, harvested 72 h later, and stained with anti-annexin V antibody and propidium iodide (BD Biosciences) as specified by the manufacturer before they were analyzed on a Beckman Coulter FC500 flow cytometer. To monitor growth of Eμ-BRD2 lymphoma cells *in vivo*, sublethally irradiated 8–9-week-old FVB female mice were injected intravenously with an equal number (5×10^4) of GFP cell-sorted primary lymphoma cells infected with lentiviral particles that express GFP along with either control sh-GFP or sh-PRMT5-1. Mice were then monitored every day for the development of lymphoma and were killed at the first appearance of clinical symptoms. All mouse experiments were performed in compliance with Federal and Institutional Animal Care and Use Committee regulations.

Real-time RT-PCR, ChIP, Western Blot, and Immunofluorescence Assays—Total RNA was isolated using TRIzol reagent, and reverse transcription was performed essentially as described previously (19, 24). To measure the mRNA levels of target genes, real-time PCR was carried out using the TaqMan system in a 10-μl reaction as described previously (17). The following primer sets and probes were used in real-time PCR analyses: *PRMT5* (forward, 5′-TATGTGGTACGGCTGCACA-3′; reverse, 5′-TGGCTGAAGGTGAAACAGG-3′; probe 31), *RBL2* (forward, 5′-TTGTTGGGTGCTTTTTATATATGC-3′; reverse, 5′-TTTCCATAAACTAAGTCCAAAGCA-3′; probe 62), *EZH2* (forward, 5′-GAAAACTTGGTGAACGCCTAA-3′; reverse, 5′-CCAACAAACTGGTCCCTTCT-3′; probe 35), *SUZ12* (forward, 5′-GGGAGACTATTCTTGATGGGAAG-3′; reverse, 5′-ACTGCAACGTAGGTCCCTGA-3′; probe 16), *EED* (forward, 5′-ATCAAATACTTTGGTGTTATTCATTC-3′; reverse, 5′-ATTGATACCTAACTGCCAACTTAAT-3′; probe 21), β-actin (forward, 5′-GGTAGACGCGATCTGTTGG-3′; reverse, 5′-GGCATGGAATCAACCTCAAC-3′; probe 2), *CASP10* (forward, 5′-GGGAAAAAGGCAGATAAGCA-3′; reverse, 5′-TCAGGACTGGGTAGCCTGAT-3′; probe 18), *DAP1* (forward, 5′-ACAAGGATGACCAGGAATGG-3′; reverse, 5′-TGACCCCAGAGATGAACACA-3′; probe 45), *HOXA5* (forward, 5′-CGTCCACGCACTCTCCTC-3′; reverse, 5′-CTGGAGTTGCTTAGGGAGTT-3′; probe 83), *HRK* (forward, 5′-CCTGGAGCGATCGTAGAAAC-3′; reverse, 5′-TGTTTCTGCAGCTGGATTTC-3′; probe 60), *CCND1* (forward, 5′-GAAGATCGTCGCCACCTG-3′; reverse, 5′-GACCTCCTCCTCGCACTTCT-3′; probe 67), *BCL3* (forward, 5′-ACTGCCTTTGTACCCCACTC-3′; reverse, 5′-GGTATAGGGGTGTAGGCAGGT-3′; probe 6), *TP53* (forward, 5′-TCCACTTCTTGTTCCCCACT-3′; reverse, 5′-AAAGACCCAAAACCCAAAATG-3′; probe 75), mouse *Prmt5* (forward, 5′-GCTGTCACCTGAGTGTCTGG-3′; reverse, 5′-GATGCTCACGCCATCATCT-3′; probe 99), mouse *Ezh2* (forward, 5′-GTGGGGAGATTATTTCTCAGGA-3′; reverse, 5′-ACGAATTTTGTTGCCCTTTC-3′; probe 35), mouse *Suz12* (forward, 5′-AAGTTCAAAACAGCACCAGTTG-3′; reverse, 5′-GCTGCATGGAAGGCAGCAGTC-3′; probe 16), mouse *Eed* (forward, 5′-CGATGGTTAGGCGATTTGAT-3′; reverse, 5′-TCGCCCAAGAATAGTCACATTA-3′; probe 88), mouse *Rbl2* (forward, 5′-TGCTGGGTGCTTTTTATATATGC-3′; reverse, 5′-GAATTGACCAGATCATCGCTAA-3′; probe 60), mouse *Dap1* (forward, 5′-TCCAGCCTTCATGGGACTAC-3′; reverse, 5′-AAAATTTGAGGAGCCCATCC-3′; probe 64), mouse *Hrk* (forward, 5′-ATGTCATTCTTGCTCACTGAGAACT-3′; reverse, 5′-GTGTAGCTCGTGCCAGGAC-3′; probe 16), mouse *Hoxa5* (forward, 5′-ACGGCCTACACTCGCTACC-3′; reverse, 5′-GTAGCGGTTGAAGTGGAATTCTT-3′; probe 32), mouse *Rb1* (forward, 5′-GCGGCAACTACAGCCTAGAG-3′; reverse, 5′-TGCGGCAAGCAACATATAAA-3′; probe 3), mouse *Ccnd1* (forward, 5′-CTCCTCTTCGCACTTCTGCT-3′; reverse, 5′-GAGATTGTGCCATCCATGC-3′; probe 67), mouse *Tp53* (forward, 5′-AGGGCTGAGACACAATCCTC-3′; reverse, 5′-GCTGAGCCCTAGCTACAAGGT-3′; probe 74), and mouse *Bcl3* (forward, 5′-CTCCAATGGCCTCCAGTC-3′; reverse, 5′-AAGCCAGGAGCATCTTTCG-3′; probe 94). To normalize mRNA levels, levels of 18 S rRNA were measured in both control and test cell lines using 1× premixed 18 S primer/probe set (Applied Biosystems). To monitor recruitment to target genes, ChIP assays were performed using cross-linked chromatin from either normal or transformed B cells as described previously (19, 24). The following primer sets and probes were used in ChIP assays: *RBL2* (forward, 5′-ATTTTTGGCCCCCTTGAA-3′; reverse, 5′-GCACCCGTAGTCTTGAGCAC-3′; probe 3), *EZH2* (forward, 5′-GGACGGGACAGACACAAGTT-3′; reverse, 5′-CCGTCCTTTGTCTGAGTGC-3′; probe 28), *SUZ12* (forward, 5′-GCAGGTTGTAGGGAGACGAA-3′; reverse, 5′-CGGTGTTTTGCGAGTCTTG-3′; probe 19), *EED* (forward, 5′-GGTACTTTCCATTCGCCAGA-3′; reverse, 5′-TCCTTGAAGATAGAAATGCAAAAAC-3′; probe 38), *CCND1* (forward, 5′-CGGGCTTTGATCTTTGCTTA-3′; reverse, 5′-TCTGCTGCTCGCTGCTACT-3′; probe 1), and *BCL3* (forward, 5′-CTGCATCCAGGATTCCAGTT-3′; reverse, 5′-GAGTGCAGCTTCTATGGTGGA-3′; probe 4).

To examine expression of PRMT5 and its downstream target genes, radioimmune precipitation assay (RIPA) extracts were prepared and analyzed by Western blot analysis as described previously (19, 27). When phospho-RB1 levels were measured, RIPA extracts were prepared in the presence of the following inhibitors: 10 mM β-glycerophosphate, 1 mM Na_3VO_4, and 50 mM NaF. Antibodies against PRMT5 and its epigenetic marks as well as SUZ12 have been described previously (17, 19, 28). Polyclonal antibodies against RB1, RBL1, RBL2, EZH2, EED, E2F1–4, E2F6, HDAC1, HDAC2, cyclin D1, CDK4, CDK6, CDKN2A/p16, CDKN1A/p21, HOXA5, HRK, BCL3, p300, and NF-κB p52 were purchased from Santa Cruz Biotechnology. Anti-EZH2, anti-caspase-10, anti-DAP1, anti-caspase-3, and anti-phospho-RB1 (Ser-780, Ser-795, and Ser-807/Ser-811) antibodies were purchased from Cell Signaling Technology, whereas anti-H3(Me_3)K27, anti-TP53, and anti-methyl-TP53 antibodies were purchased from Abcam. Both anti-H3K9ac and anti-H3K14ac antibodies were purchased from EMD Millipore, and anti-β-actin antibody was purchased from Sigma-Aldrich. Immunofluorescence experiments were performed as described previously (17).

Immunohistochemistry—To evaluate PRMT5 expression in NHL patient samples, formalin-fixed primary tumor samples collected from 53 MCL patients (34 common, 14 blastoid, and 5 pleomorphic histologic subtypes) and 62 DLBCL patients (29 GCB and 33 ABC histologic subtypes) were used. Studies that

examined expression of PRMT5, EZH2, and their associated epigenetic marks as well as RB1, phospho-RB1 (Ser-795), and RBL2 levels were performed on a second tissue microarray (TMA) generated from formalin-fixed, paraffin-embedded tissue samples corresponding to 16 MCL and 18 DLBCL cases, which were included in the original TMA studied for PRMT5 expression. The second TMA used in these experiments was constructed as reported previously (29). All cases were retrieved from the archives of the Hematopathology Unit, Department of Experimental, Diagnostic and Specialty Medicine (DIMES), University of Bologna. MCL cases were classified in the three morphologic variants according to the World Health Organization classification (4): nine common variant, four blastoid variant, and three pleomorphic variant. DLBCL samples were classified as GCB- and ABC-like according to the Hans algorithm (31): 10 GCB-DLBCL and 8 ABC-DLBCL. Paraffin-embedded sections (4-μm thick) were cut from TMA blocks, dewaxed, and submitted to antigen retrieval by heating in Dako PT Link (PT100/PT101, DakoCytomation, Glostrup, Denmark). Slides were placed in EnVision FLEX high pH target retrieval solution (K8004, DakoCytomation) at 92 °C for 5 min and then incubated at room temperature with the following antibodies: anti-PRMT5 (1:120 dilution), anti-H3(Me_2)R8 (1:180), anti-H4(Me_2)R3 (1:960), anti-EZH2 (1:120), anti-H3(Me_3)K27 (1:40), anti-RB1 (1:120), anti-phospho-RB1 (Ser-795; 1:30), and anti-RBL2 (1:120). All antibodies were diluted with Dako REAL antibody diluent (S2022, DakoCytomation). Immunostaining was performed using the Alkaline REAL alkaline phosphatase/RED rabbit/mouse detection system (K5005, DakoCytomation). Finally, sections were counterstained with hematoxylin. For negative controls, primary antibodies were omitted. A cutoff of staining of >30% of the examined cells was assigned as a positive score, according to formerly defined criteria (29). The staining intensity regarded as weak, moderate, or strong was also recorded. Immunohistochemical preparations were visualized using an Olympus BX41 microscope equipped with an Olympus UPlanFI 40×/0.75 numerical aperture objective, and images were captured using an Olympus CAMEDIA C-3040 Zoom digital camera.

Statistical Analysis—Results are expressed as means ± S.D. unless specified otherwise. Paired *t* tests and analysis of variance were used to generate *p* values for comparisons between two groups and when multiple samples within different groups were used, respectively.

RESULTS

Expression of PRMT5 and PRC2 Inversely Correlates with RBL2 Levels—We previously showed that PRMT5 epigenetically silences *RBL2* expression and that its knockdown inhibits lymphoma cell growth (17, 18). However, the molecular mechanisms by which PRMT5 promotes lymphoma cell growth and survival remain unclear. EZH2, the catalytic subunit of PRC2, has been shown to be highly expressed in metastatic prostate and breast cancer as well as in lymphoma (32–34). What is more interesting is that *EZH2* is a downstream target gene of E2F transcription factors (23). To investigate the relationship between PRMT5, RBL2, and PRC2, we examined their expression in three different types of NHL cells, including pre-GCB MCL (Mino and JeKo), GCB-DLBCL (Pfeiffer and Toledo), and post-GCB ABC-DLBCL (SUDHL-2 and OCI-Ly3) (Fig. 1*A*). Both PRMT5 and PRC2 were overexpressed, whereas RBL2 levels were suppressed in NHL cells compared with normal resting or activated $CD19^+$ B cells. In accord with these results, real-time RT-PCR revealed that the mRNA levels of PRC2 components were elevated by 1.6–5-fold ($p < 10^{-3}$) and that *RBL2* mRNA levels were suppressed by 2–10-fold ($p < 10^{-3}$) in NHL cell lines (Fig. 1*B*).

Using normal B cells as a control and one representative cell line from each NHL cell type, we tested whether PRMT5 and its epigenetic marks can be detected at the *RBL2* promoter (−85 to −16) (Fig. 1*C*). Both PRMT5 and its induced marks were enriched by 2.5–8-fold ($p < 10^{-3}$) at the *RBL2* promoter region in all three NHL cell lines. We also analyzed the global levels of PRMT5, PRC2, and RBL2 by immunofluorescence (Fig. 1*D*). Consistent with the Western blot results, PRMT5, PRC2, and their associated marks were elevated in NHL cell lines. In contrast, RBL2 protein levels were high in normal B cells and undetectable in NHL cells. These observations suggest that PRMT5, through its ability to suppress RBL2, promotes PRC2 expression.

PRMT5 Knockdown Results in RBL2 Derepression and PRC2 Silencing—To determine whether PRMT5 can affect RBL2 and PRC2 expression, JeKo, Pfeiffer, and SUDHL-2 cells were infected with lentivirus that expresses either control sh-GFP or two *PRMT5*-specific shRNAs (sh-PRMT5-1 and sh-PRMT5-2), and total RNA and RIPA extracts were analyzed (Fig. 2). Both RNA and Western blot analyses showed that PRMT5 knockdown triggered *RBL2* derepression and PRC2 silencing (Fig. 2, *A* and *B*). Because both *PRMT5*-specific shRNAs gave similar results, we performed further experiments using only sh-PRMT5-1. To further confirm our Western blot results, we measured the global levels of PRMT5, RBL2, and PRC2 by immunofluorescence (Fig. 2*C*). Our findings show that although PRMT5, PRC2, and their induced epigenetic marks were elevated, RBL2 expression was suppressed in control uninfected and sh-GFP-infected Pfeiffer cells. When PRMT5 was knocked down, RBL2 expression was restored, and PRC2 levels were decreased. Similar results were observed by immunofluorescence in JeKo and SUDHL-2 cells (data not shown). Furthermore, when we measured the proliferation of control sh-GFP- and sh-PRMT5-1-infected NHL cells, there was a clear inhibition of growth in cells in which PRMT5 was knocked down (Fig. 3*A*), which was accompanied by enhanced cell death as determined by increased annexin V staining (Fig. 3*B*) and caspase-3 activation (Fig. 3*C*). In light of these results, we tested whether PRMT5 knockdown could affect expression of PRC2 downstream target genes, which regulate cell death. On the basis of previously published ChIP-Seq data (35, 36), we selected four PRC2 pro-apoptotic target genes, including *CASP10*, an initiator caspase that activates CASP3 and CASP7 (37); *DAP1*, which acts as a positive mediator of apoptosis (38); *HOXA5*, a transcription factor silenced in >60% of breast carcinomas and whose re-expression induces apoptosis (39); and *HRK*, which activates cell death through inhibition of Bcl-2 and Bcl-x_L (40). Real-time RT-PCR analysis showed that despite the fact that the kinetics of reactivation for PRC2 pro-apoptotic target genes varied within and between NHL cell lines, all four target genes were derepressed by 1.5–4-fold ($p < 10^{-3}$) in PRMT5 knockdown cells (Fig. 3*D*). Similar results were observed in JeKo and SUDHL-2 cells (data not shown). Importantly, tran-

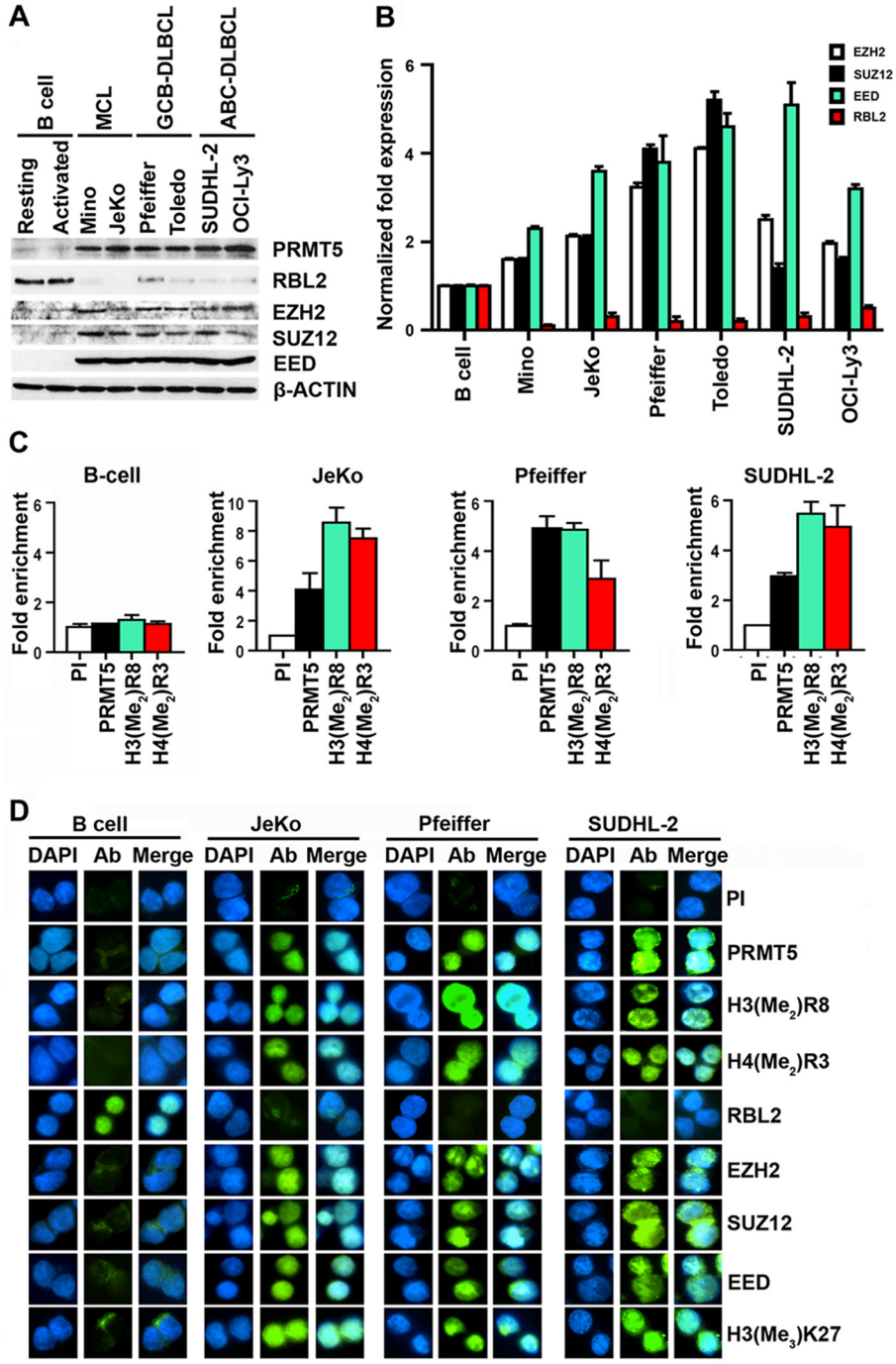

FIGURE 1. **Overexpressed PRMT5 epigenetically silences *RBL2* and promotes PRC2 expression in patient-derived NHL cell lines.** *A*, RIPA extracts (20 μg) from normal B (resting or activated), pre-GCB MCL (Mino and JeKo), GCB-DLBCL (Pfeiffer and Toledo), and post-GCB ABC-DLBCL (SUDHL-2 and OCI-Ly3) cells were analyzed by immunoblotting using the indicated antibodies. Anti-β-actin antibody was used as control. *B*, the levels of *RBL2*, *EZH2*, *SUZ12*, and *EED* mRNAs were measured in normal and transformed B cells by real-time RT-PCR using gene-specific primers and probe sets. This experiment was conducted three times in triplicate, and 18 S rRNA was used as internal control. *C*, ChIP experiments were performed on cross-linked chromatin from either normal or transformed B cells using preimmune (*PI*), anti-PRMT5, anti-H3(Me_2)R8, and anti-H4(Me_2)R3 antibodies. ChIP assays were carried out twice in triplicate. -Fold enrichment with each antibody was calculated relative to the preimmune sample. *D*, normal resting and transformed B cells were fixed and incubated with the indicated primary antibodies (*Ab*), and FITC-labeled goat anti-rabbit antibody was used to detect PRMT5, PRC2, and their marks as well as RBL2. DAPI was used to stain nuclei. Pictures were taken at [100 magnification, and data in each graph are represented as means $\pm$ S.D.

scriptional derepression correlated with increased CASP10, DAP1, HOXA5, and HRK protein expression (Fig. 3*E*). Collectively, these results indicate that PRMT5 promotes NHL cell growth and survival by indirectly suppressing expression of cell death-inducing genes.

Reduced PRMT5 Expression Restores Recruitment of RB1/RBL2-HDAC2 Repressor Complexes to the EZH2, SUZ12, and EED Promoters—Having found that RBL2 derepression correlates with PRC2 silencing and knowing that expression of EZH2 and EED is controlled by E2Fs in human fibroblasts (23), we

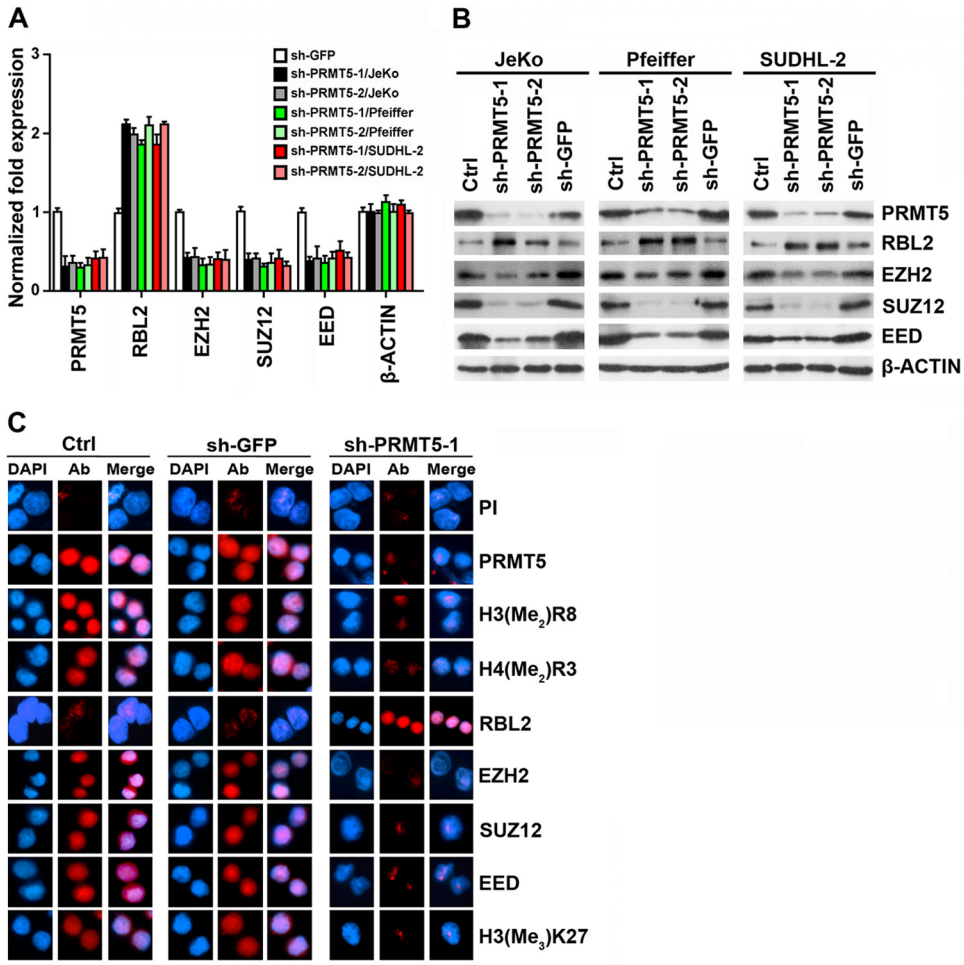

FIGURE 2. **PRMT5 knockdown results in RBL2 reactivation and PRC2 suppression.** *A*, total RNA isolated from JeKo, Pfeiffer, and SUDHL-2 cells infected with control sh-GFP, sh-PRMT5-1, or sh-PRMT5-2 lentivirus was analyzed by real-time RT-PCR 72 h post-infection as described in the legend to Fig. 1*B*. Data are represented as means ± S.D. *B*, RIPA extracts (20 μg) were prepared from control uninfected (*Ctrl*) and infected (sh-GFP, sh-PRMT5-1, or sh-PRMT5-2) NHL cell lines and analyzed by immunoblotting using the indicated antibodies. Anti-β-actin antibody was included to show equal loading. *C*, immunofluorescence of control uninfected, sh-GFP-infected, and sh-PRMT5-1-infected Pfeiffer cells was carried out as described in the legend to Fig. 1*D*, except that TRITC-labeled goat anti-rabbit antibody was used as secondary antibody (*Ab*).

sought to assess the role of RB-E2F in PRC2 regulation in NHL cells. First, we examined the promoter regions of *EZH2*, *SUZ12*, and *EED* (−1 to +0.5 kilobase pairs) for the presence of E2F-binding sites using TESS software (41). Our analysis indicated that there are 15 and 17 E2F-binding sites in the *EZH2* and *SUZ12* promoters, respectively, whereas the *EED* promoter region contains only one E2F-binding site. Using antibodies that recognize individual E2F transcription factors, we performed ChIP assays using cross-linked chromatin from both normal and transformed B cells (Fig. 4*A*). Binding of E2F1–4 was enriched by 2–9-fold ($p < 10^{-3}$) in the promoter region of PRC2 components in normal B cells; however, only E2F1, E2F3, and E2F4 showed increased binding in NHL cells in comparison with the preimmune control. We also examined the recruitment of pocket proteins and discovered that association of RB1 and RBL2 was enhanced by 2.5–6-fold ($p < 10^{-4}$) in normal B cells but not in NHL cells. Because pocket proteins are known to repress E2F-driven genes through direct interaction with and recruitment of histone deacetylases (22), we also evaluated HDAC2 recruitment and acetylation of H3K9 and H3K14 in the promoter region of PRC2 subunits. Consistent with RB1 and RBL2 binding, recruitment of HDAC2 was increased by 2.5–5.5-fold ($p < 10^{-3}$) in normal B cells but not in NHL cells, suggesting that deficiency in recruitment of RB1/RBL2-HDAC2 repressor complexes contributes to PRC2 up-regulation in NHL cells.

To evaluate the role of PRMT5 in PRC2 regulation, we knocked down its expression and monitored the recruitment of relevant E2F and RB proteins to the promoter region of PRC2 components in both control sh-GFP and PRMT5 knockdown Pfeiffer cells (Fig. 4*B*). Our results show that although there was no change in binding of E2Fs, there was a 2–4-fold ($p < 10^{-3}$) enhancement of RB1 and RBL2 recruitment in PRMT5 knockdown cells compared with control cells. HDAC2 recruitment was also increased and was accompanied by H3K9/H3K14 deacetylation in the promoter region of PRC2 components in PRMT5 knockdown cells, highlighting the important role played by RB1/RBL2-HDAC2 repressor complexes in PRC2 regulation. Similar results were observed in JeKo and SUDHL-2 cells (data not shown). These results show that PRMT5 inhibition reactivates RB1/RBL2 and suppresses PRC2 expression.

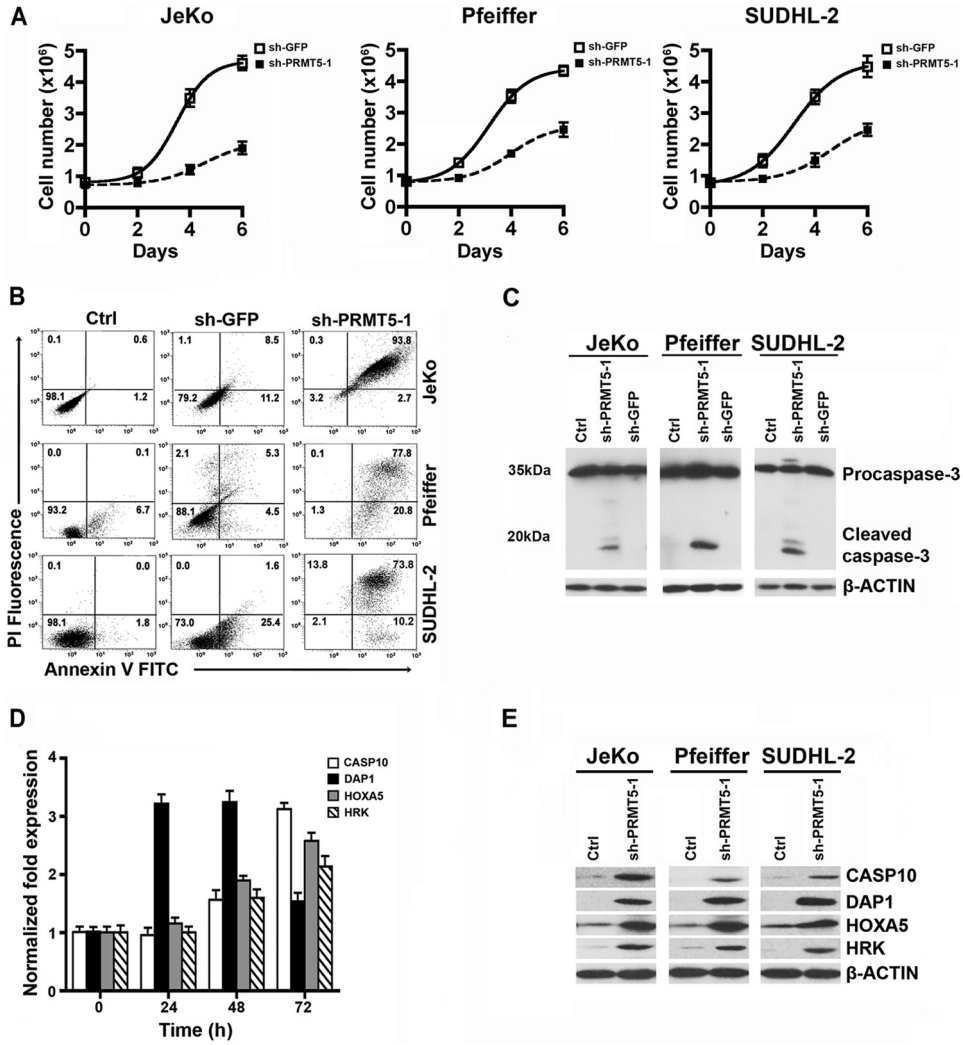

FIGURE 3. **Reduced PRMT5 expression inhibits NHL cell growth and induces cell death.** *A*, proliferation of sh-GFP- and sh-PRMT5-1-infected NHL cells was determined by seeding 8×10^5 cells in each well and counting the number of viable cells every 2 days for 6 days. This experiment was conducted twice in triplicate. *B*, apoptosis of uninfected and infected JeKo, Pfeiffer, and SUDHL-2 cells was assessed by FACS analysis using propidium iodide (*PI*)/annexin V staining. *C*, JeKo, Pfeiffer, and SUDHL-2 cells were infected with either control sh-GFP or sh-PRMT5-1 lentivirus, and activation of caspase-3 was analyzed by Western blotting. Uninfected cells were used as control (*Ctrl*). *D*, total RNA was prepared at the indicated times from control sh-GFP- or sh-PRMT5-1-infected Pfeiffer cells, and expression of *CASP10*, *DAP1*, *HOXA5*, and *HRK* was analyzed by real-time RT-PCR as described in the legend to Fig. 1*B*. *E*, expression of PRC2 pro-apoptotic targets in JeKo, Pfeiffer, and SUDHL-2 cells infected with either sh-GFP or sh-PRMT5-1 was evaluated by Western blotting using RIPA extracts (20 μg) as described in the legend to Fig. 2*B*. Samples used to analyze expression of CASP10, HOXA5, and HRK were harvested 72 h post-infection, whereas DAP1 expression was analyzed 48 h post-infection. Data in each graph are represented as means ± S.D.

PRMT5 Up-regulates Cyclin D1-CDK4/6 Proliferative Signaling in NHL Cells—A major growth regulatory network that is altered in various cancer cells is the cyclin D1-CDK4/6-RB pathway, which controls the E2F-driven transcriptome (42, 43). We have found by ChIP assay that RB1 recruitment is enhanced to the promoter region of PRC2 components in PRMT5 knockdown cells (Fig. 4), suggesting that RB1 has regained its transcriptional inhibitory activity, which may occur only if RB1 becomes hypophosphorylated. To test this hypothesis, we examined the relationship between PRMT5 and phospho-RB1 in NHL cells (Fig. 5*A*). We discovered that RB1 phosphorylation at multiple sites (Ser-780, Ser-795, and Ser-807/Ser-811) was more abundant in NHL cells than in normal B cells. We also analyzed expression of cyclin D1, CDK4, CDK6, and their inhibitors and found that despite increased expression of CDKN2A/p16 and or CDKN3/p21, RB1 was still hyperphosphorylated, suggesting that cyclin D1-CDK4/6 complexes are functional in NHL cells.

To determine whether PRMT5 is involved in promoting cyclin D1-CDK4/6 signaling, we inhibited its expression by shRNA-mediated knockdown in JeKo, Pfeiffer, and SUDHL-2 cells and monitored cyclin D1-CDK4/6 expression as well as RB1 phosphorylation (Fig. 5*B*). In all three NHL cell types, PRMT5 inhibition led to decreased cyclin D1 expression. In addition, we noticed a modest decrease in CDK6 levels, whereas CDK4 was unaffected. To measure the activity of cyclin D1-CDK4/6 complexes, we monitored the levels of phospho-RB1 using three distinct antibodies. In agreement with decreased cyclin D1 protein levels, RB1 phosphorylation was inhibited in PRMT5 knockdown NHL cell lines. These results suggest that cyclin D1-CDK4/6-mediated RB1 phosphorylation depends on the presence of PRMT5.

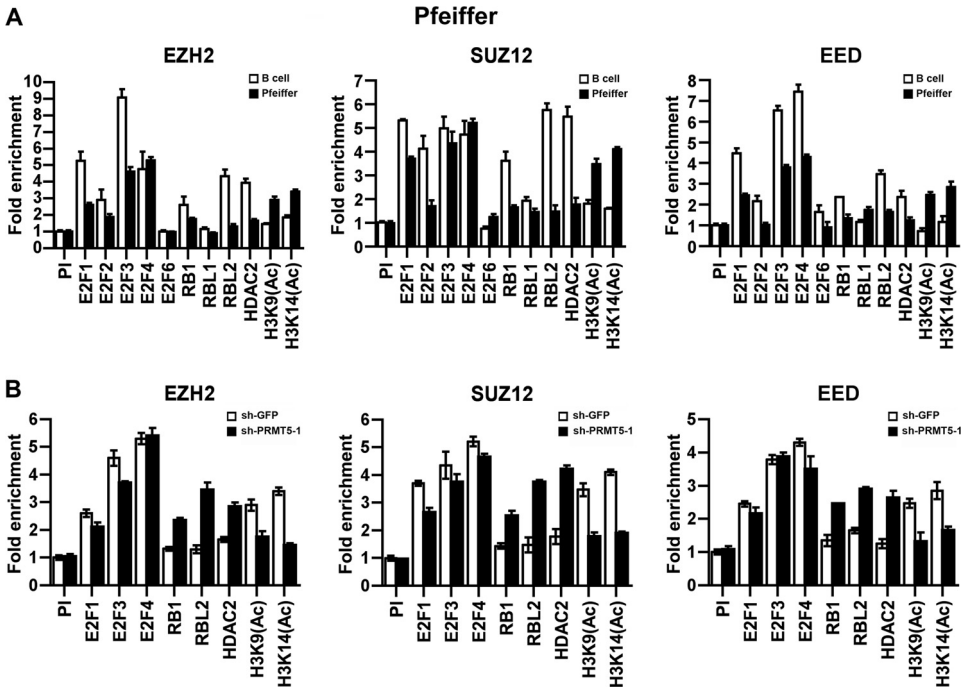

FIGURE 4. **PRMT5 inhibition restores recruitment of RB1/RBL2-HDAC2 repressor complexes to the *EZH2*, *SUZ12*, and *EED* promoters.** *A*, cross-linked chromatin from either normal B or Pfeiffer cells was immunoprecipitated using the indicated antibodies, and promoter sequences of PRC2 subunits were detected as described in the legend to Fig. 1*C*. *B*, real-time ChIP assays were carried out using cross-linked chromatin from either sh-GFP- or sh-PRMT5-1-infected Pfeiffer cells. -Fold enrichment with each antibody was calculated relative to the preimmune (*PI*) sample. The data points in each graph show the average from two independent experiments in triplicate and are plotted as means ± S.D.

To shed more light on the mechanism by which PRMT5 inhibition triggers cyclin D1 down-regulation, we measured cyclin D1 mRNA and protein expression at different time points after PRMT5 knockdown (Fig. 5, *C* and *D*). Cyclin D1 mRNA levels begun to drop as early as 36 h, whereas cyclin D1 protein expression decreased 48 h post-infection in knockdown Pfeiffer cells. Similar results were observed in JeKo and SUDHL-2 cells (data not shown). Prior work showed that the NF-κB p52-BCL3 complex drives cyclin D1 expression in H1299 and U2OS cells and that TP53-mediated inhibition of *BCL3* results in cyclin D1 transcriptional repression (44). However, the mechanism by which TP53 represses *BCL3* remains unknown. The same report also showed that loss of BCL3 expression promotes formation of NF-κB p52-HDAC1 complexes, which actively repress cyclin D1 transcription.

To investigate if cyclin D1 expression is regulated via a similar mechanism in NHL cells, we measured *TP53* and *BCL3* mRNA and protein expression before and after PRMT5 knockdown. We found that *BCL3* transcription was inhibited 36 h post-infection and that this correlated with decreased BCL3 protein expression in knockdown Pfeiffer cells (Fig. 5, *C* and *D*). Decreased expression of BCL3 was also observed in knockdown SUDHL-2 cells (data not shown). However, because JeKo cells are TP53-deficient despite detectable *TP53* mRNA levels (Ref. 45 and data not shown), we analyzed cyclin D1, *TP53*, and *BCL3* mRNA and protein expression as well as RB1 phosphorylation in Mino cells infected with lentivirus that expresses either sh-GFP or sh-PRMT5-1 (data not shown). Consistent with our findings in Pfeiffer and SUDHL-2 cells, expression of cyclin D1 was inhibited in PRMT5 knockdown Mino cells, as was RB1 phosphorylation (data not shown). Moreover, *BCL3* mRNA and protein expression was decreased 48 h post-infection (data not shown). Remarkably, *TP53* mRNA and protein expression increased 36–48 h after PRMT5 knockdown in Pfeiffer and SUDHL-2 cells but not in Mino cells (data not shown), which are known to express high levels of TP53 (45), suggesting that TP53 is involved in *BCL3* transcriptional repression in NHL cells.

To verify that TP53 is directly involved in *BCL3* transcriptional repression, we monitored its recruitment to the *BCL3* promoter in Pfeiffer cells (Fig. 5*E*) and in Mino and SUDHL-2 cells (data not shown). TP53 binding was enhanced by 2–4-fold ($p < 10^{-3}$) in both control sh-GFP and PRMT5 knockdown NHL cells, suggesting that *BCL3* transcriptional repression does not depend on TP53 protein induction. Because TP53 is methylated at Lys-372 by KMT7 (SET7/9), and it is known that this modification enhances TP53 transcriptional activity (46), we measured its levels as well as presence at the *BCL3* promoter before and after PRMT5 knockdown. In all three NHL cell lines, TP53K372 methylation was reduced 48–72 h post-infection (Fig. 5*D*), as was binding of Lys-372-methylated TP53 to the *BCL3* promoter, which showed a maximal decline 60–72 h post-infection (Fig. 5*E*), indicating that loss of TP53K372 methylation correlates with decreased *BCL3* promoter activity. We also monitored recruitment of p300 and HDAC2 and found that their binding correlated with TP53-mediated *BCL3* transcriptional activation and repression, respectively.

Given that BCL3 down-regulation coincided with cyclin D1 suppression, we examined recruitment of NF-κB p52, BCL3, and HDAC1 to the cyclin D1 promoter in all three NHL cell types (Fig. 5*F* and data not shown). Our findings indicate that even though NF-κB p52 binding did not change over time,

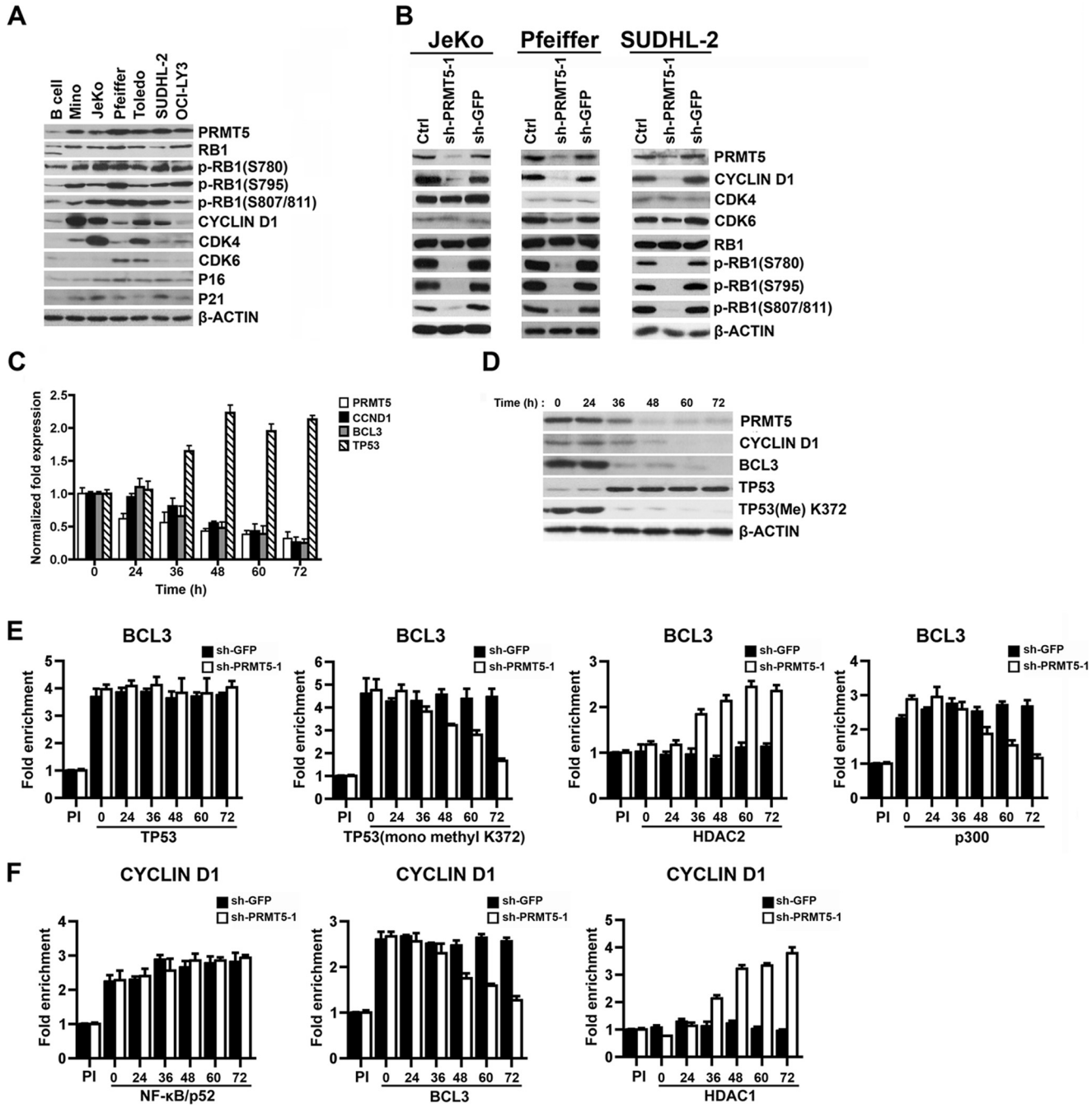

FIGURE 5. **PRMT5 inhibition antagonizes cyclin D1-CDK4/6 signaling.** *A*, RIPA extracts (20 μg) from normal and transformed B cells were examined by immunoblotting using the indicated antibodies. *p-RB1*, phospho-RB1. *B*, JeKo, Pfeiffer, and SUDHL-2 cells were infected with either control sh-GFP or sh-PRMT5-1 lentivirus, and RIPA extracts (20 μg) were analyzed by Western blotting. Uninfected cells were used as control (*Ctrl*). *C*, Pfeiffer cells were infected with sh-PRMT5-1 virus, and the mRNA levels of *PRMT5*, cyclin D1, *BCL3*, and *TP53* were measured by real-time RT-PCR at different time points. For comparison, the steady-state levels of the target genes examined were determined before infection and are shown at time point 0 h. *D*, RIPA extracts (20 μg) were analyzed by Western blot analysis using the indicated antibodies, except for the anti-TP53 Western blot, where 100 μg of RIPA was analyzed instead. ChIP experiments were performed at the indicated time points on cross-linked chromatin from Pfeiffer cells infected with either control sh-GFP or sh-PRMT5-1 using the indicated antibodies. *E* and *F*, both real-time RT-PCR and ChIP assays were conducted twice in triplicate, and the data points in each graph are represented as means ± S.D. *PI*, preimmune.

BCL3 recruitment showed a steady decrease that started at 36 h and became maximal at 72 h post-infection in PRMT5 knockdown NHL cells. Concomitantly, HDAC1 recruitment to the cyclin D1 promoter increased gradually between 36 and 72 h post-infection. Collectively, these results suggest that PRMT5 promotes cyclin D1-CDK4/6 proliferative signaling through modulation of the TP53/NF-κB p52/BCL3 pathway.

PRMT5 Overexpression Correlates with RB1/RBL2 Inactivation and Enhanced PRC2 Expression in NHL Patient Samples—Having established that PRMT5 is overexpressed in NHL cell lines and that it up-regulates PRC2 expression through inactivation of RB1 and RBL2, we wanted to verify our findings in NHL patient samples. First, we evaluated PRMT5 expression in primary lymphoma samples collected from patients with MCL

(n = 53), GCB-DLBCL (n = 29), and ABC-DLBCL (n = 33) (Table 1). PRMT5 was abundantly expressed in the majority of MCL, with histologic subtypes showing 85% positivity in common MCL, 93% in blastoid variant tumors, and 100% in pleomorphic variant tumors. When we examined DLBCL samples, 97% of GCB-DLBCL and 100% of ABC-DLBCL showed PRMT5 overexpression.

We next explored the expression profile of PRMT5, EZH2, their associated marks, RB1, and RBL2 in primary tumor samples collected from patients with MCL, GCB-DLBCL, and ABC-DLBCL. However, because of limitation of tissue availability on most TMAs, these studies were performed on a newly constructed TMA as described previously (29). Both PRMT5 and its induced H3(Me_2)R8 and H4(Me_2)R3 marks were present in all cases of MCL, GCB-DLBCL, and ABC-DLBCL (Fig. 6 and Table 2). EZH2 and H3(Me_3)K27 were strongly positive in 100% of MCL and ABC-DLBCL specimens. All GCB-DLBCL samples showed EZH2 expression, with 80% of the clinical samples showing global staining for H3(Me_3)K27. Interestingly, all lymphoma histologic subtypes showed a diffuse and strong nuclear staining for RB1 and phospho-RB1 (Ser-795), which were detected in 88% of MCL samples and in 100% of GCB-DLBCL and ABC-DLBCL specimens. Consistent with our findings in patient-derived NHL cell lines, RBL2 was either silenced or weakly expressed in all primary tumor specimens. These results support our cell line data and further demonstrate the positive correlation between PRMT5, phospho-RB1, and PRC2 and the inverse correlation between PRMT5 and RBL2.

PRMT5 Knockdown Results in Enhanced Mouse Primary Lymphoma Cell Death—To demonstrate the relevance of PRMT5 in controlling lymphoma cell growth and survival, we examined its expression in mouse primary lymphoma cells derived from the Eμ-BRD2 transgenic mouse, which expresses BRD2 (double bromodomain-containing protein 2) under the control of a murine immunoglobulin heavy chain promoter-enhancer construct (26). A key feature of Eμ-BRD2 transgenic mice is that they develop an aggressive B cell lymphoma similar to human DLBCL as determined by transcriptome analysis (47). In light of our results, we reasoned that PRMT5 expression might be altered in Eμ-BRD2 primary lymphoma cells and that it might up-regulate PRC2 expression through inactivation of the RB-E2F pathway. Therefore, we examined expression of PRMT5 and its target genes in control $CD19^+$ B cells and Eμ-BRD2 primary lymphoma cells (Fig. 7, *A* and *B*). Real-time RT-PCR and Western blot analyses revealed that PRMT5 and PRC2 expression was elevated in primary lymphoma cells and inversely correlated with RBL2 levels. We also found a positive

TABLE 1

Expression of PRMT5 in primary lymphoma tumor specimens

MCL has been classified as three morphologic variants according to the World Health Organization (30). DLBCL has been classified as GCB and ABC phenotypes according to the Hans algorithm (31).

Lymphoma histology	Total cases	PRMT5-positive	PRMT5-negative
MCL			
Common	34	29	5
Blastoid	14	13	1
Pleomorphic	5	5	0
DLBCL			
GCB	29	28	1
ABC	33	33	0

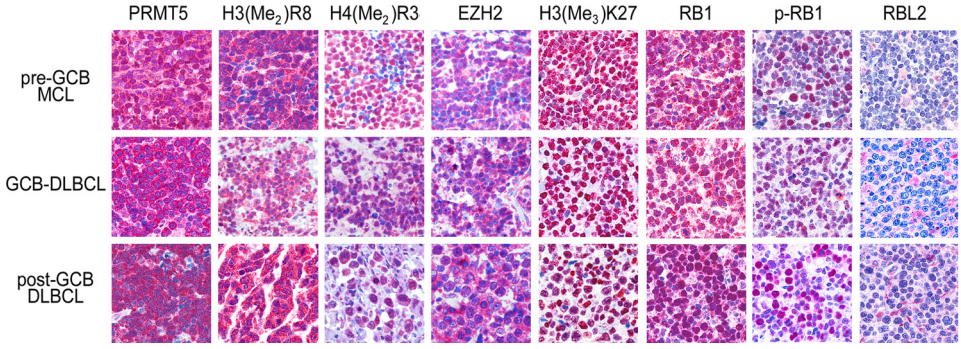

FIGURE 6. **PRMT5 overexpression correlates with enhanced levels of PRC2 and phospho-RB1 and *RBL2* suppression in NHL clinical samples.** Overexpression of PRMT5 in MCL (n = 16), GCB-DLBCL (n = 10), and ABC-DLBCL (n = 8) primary tumors is associated with H3(Me_2)R8 and H4(Me_2)R3 hypermethylation, constitutive phosphorylation of RB1 (Ser-795), silencing of RBL2, and increased PRC2 expression and the associated H3(Me_3)K27 mark. Representative panels from the three tumor cell types are shown for each antibody. Immunohistochemical staining was performed on a TMA constructed from evaluable cases as described under "Experimental Procedures."

TABLE 2

Summary of PRMT5, RB1, RBL2, and EZH2 immunohistochemical staining in clinical samples

Immunohistochemical results indicate the number of positive cases/number of evaluable cases. MCL has been classified as three morphologic variants according to the World Health Organization (30). DLBCL has been classified as GCB and ABC phenotypes according to the Hans algorithm (31).

Lymphoma histology	PRMT5	H3R8me2	H4R3me2	EZH2	H3K27me3	RB1	Phospho-RB1	RBL2
MCL								
Common	9/9	9/9	9/9	9/9	9/9	9/9	8/9	2[a]/9
Blastoid	4/4	4/4	4/4	4/4	4/4	4/4	3/4	0/4
Pleomorphic	3/3	3/3	3/3	3/3	3/3	3/3	3/3	1[a]/3
DLBCL								
GCB	10/10	8/10	10/10	9/10	8/10	10/10	10/10	5[b]/9
Post-GCB	8/8	8/8	7/8	6/8	8/8	8/8	8/8	1[a]/8

[a] Faint positivity.
[b] Faint positivity in three cases.

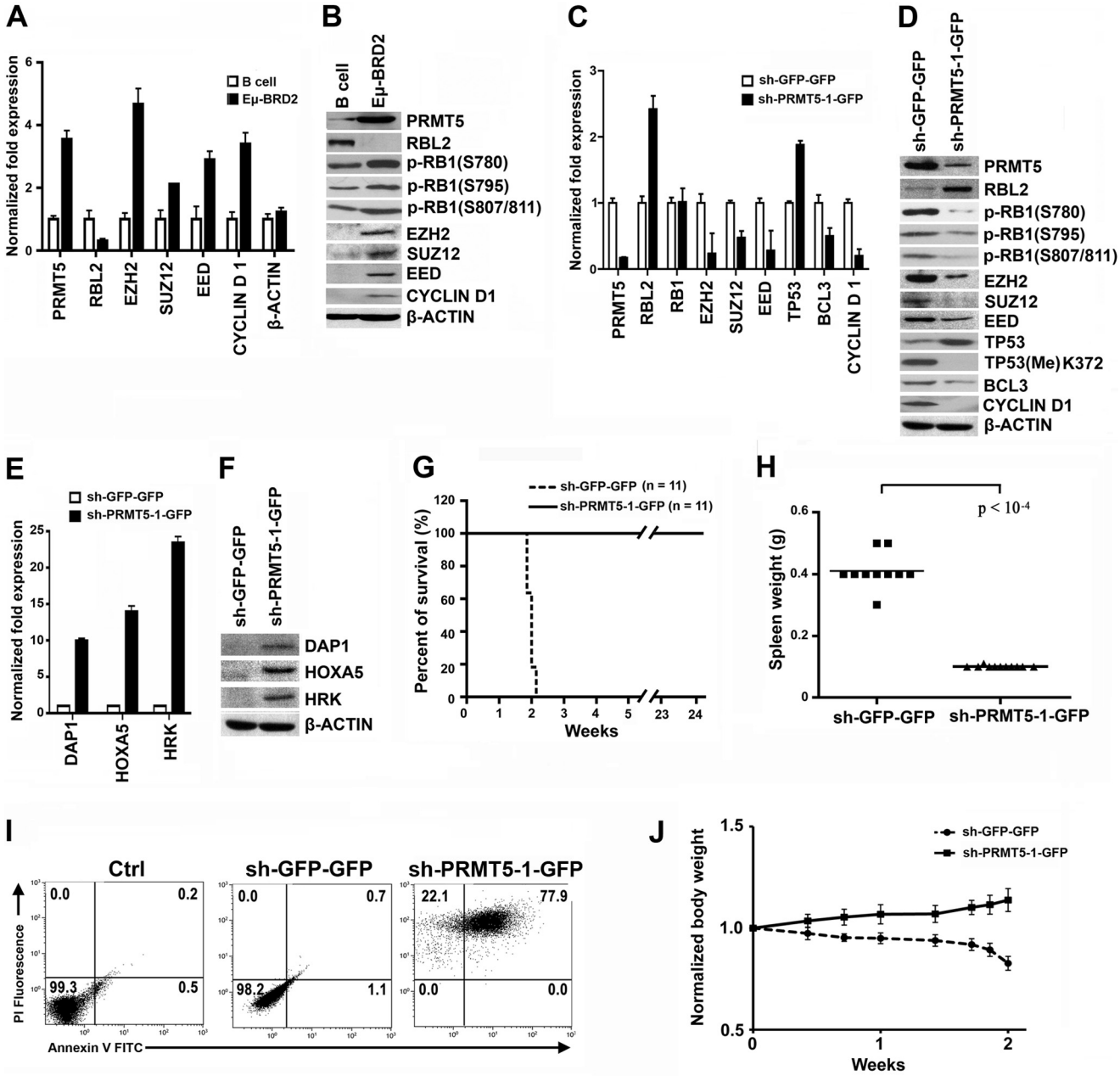

FIGURE 7. **Expression of PRMT5, PRC2, and cyclin D1 is elevated in mouse primary lymphoma cells.** *A*, real-time RT-PCR was performed on total RNA from normal B and Eμ-BRD2 cells, and the levels of the indicated target genes were determined as described in the legend to Fig. 1*B*. β-Actin mRNA levels are shown as a control. *B*, RIPA extracts (40 μg) were analyzed by immunoblotting using the indicated antibodies. Total RNA (*C* and *E*) and RIPA extracts (*D* and *F*) were collected 48 h after infection, and the levels of the indicated target genes and proteins were determined. G, Kaplan-Meier curve showing survival of mice injected with activated Eμ-BRD2 cells infected with either control sh-GFP-GFP or sh-PRMT5-1-GFP lentivirus. Eμ-BRD2 cells were activated for 24 h by adding recombinant human interleukin-4 (15 ng/ml) and goat anti-human IgG + IgM (15 μg/ml) before infection with control sh-GFP-GFP or sh-PRMT5-1-GFP lentivirus. GFP-positive control and test cells were purified by FACS analysis and injected into sublethally irradiated FVB mice. *H*, weight of spleens isolated from mice shown in *G*. *I*, activated Eμ-BRD2 lymphoma cells were infected with either control sh-GFP-GFP or sh-PRMT5-1-GFP lentivirus, stained with propidium iodide (*PI*) and annexin V 72 h later, and analyzed by FACS analysis as described in the legend to Fig. 3*B*. Activation of Eμ-BRD2 cells was carried out by adding 15 ng/ml recombinant human interleukin-4 and 15 μg/ml goat anti-human IgG + IgM. *J*, weights of individual mice ($n = 11$/group) injected with either sh-GFP-GFP- or sh-PRMT5-1-GFP-infected lymphoma cells were monitored for 2 weeks and normalized to one at day 0. The average weight for each group is plotted as means ± S.D.

correlation between enhanced cyclin D1 expression and RB1 phosphorylation.

To evaluate the contribution of PRMT5 to PRC2 regulation in Eμ-BRD2 primary lymphoma cells, we knocked down its expression and measured the levels of RB1, RBL2, and PRC2 components as well as RB1 phosphorylation 72 h post-infection (Fig. 7, *C* and *D*). We found that PRC2 expression was reduced and correlated with RBL2 derepression and RB1 hypophosphorylation. We also found that cyclin D1 expression was inhibited at the transcriptional level and correlated with *BCL3* repression. More importantly, TP53K372 methylation was also decreased in PRMT5 knockdown primary lymphoma cells, suggesting that the mechanism of cyclin D1 regulation is conserved between human and mouse lymphoma cells. Consistent with decreased PRC2 levels, expression of DAP1, HOXA5, and HRK was increased in PRMT5

knockdown cells and was accompanied by enhanced cell death (Fig. 7, *E*, *F*, and *I*).

Because Eμ-BRD2 primary tumor cells induce an aggressive lymphoma that results in animal death within 2–3 weeks, we assessed the impact of PRMT5 knockdown on their growth and survival *in vivo*. Mouse primary lymphoma cells were infected with either control sh-GFP-GFP or sh-PRMT5-1-GFP lentivirus, and GFP-positive cells were purified 24–36 h post-infection by FACS analysis and immediately injected into sublethally irradiated FVB mice (Fig. 7*G*). The Kaplan-Meier survival curve showed that mice ($n = 11$) injected with control sh-GFP lymphoma cells succumbed to disease within 13–15 days and showed splenomegaly (Fig. 7*H*) as well as weight loss (Fig. 7*J*). In addition, necropsy of sick animals showed evidence of lymphoma in peripheral blood, bone marrow, lymph nodes, lungs, liver, kidneys, and pancreas (data not shown). In contrast, mice injected with sh-PRMT5-1-GFP lymphoma cells ($n = 11$) survived for >24 weeks without any clinical symptoms ($p < 10^{-4}$). These results show that PRMT5 inhibition results in primary lymphoma cell growth arrest and death.

DISCUSSION

Understanding how cancer cells acquire the ability to survive and proliferate uncontrollably requires the discovery of mechanisms that contribute to aberrant expression of target genes that in turn adversely affect critical regulatory checkpoints. We have determined that PRMT5 is overexpressed in three different types of NHL cell lines and clinical samples and that it up-regulates PRC2 expression through inactivation of RB1 and RBL2. We have demonstrated that PRMT5 epigenetically silences RBL2 and indirectly contributes to RB1 inactivation by phosphorylation. Consequently, these events result in decreased recruitment of RB1/RBL2-HDAC2 repressor complexes to the *EZH2*, *SUZ12*, and *EED* promoters, augmenting PRC2 expression and function in NHL cells. We have shown that PRMT5 knockdown reactivates the RB1/RBL2-E2F tumor suppressor pathway and antagonizes cyclin D1-CDK4/6 signaling in both NHL cell lines and mouse primary lymphoma cells. Further investigation revealed that although the levels of PRMT5, PRC2, and their induced epigenetic marks are enhanced, both RB1 and RBL2 are inactivated in NHL clinical samples. In agreement with our findings in NHL cell lines and patient samples, we have shown that PRMT5 overexpression results in enhanced PRC2 and cyclin D1 levels in mouse primary lymphoma cells and that PRMT5 knockdown restores RB1 and RBL2 tumor suppressor activity, induces expression of pro-apoptotic target genes, and inhibits tumor cell growth and survival in an aggressive DLBCL mouse model.

Our findings show that reactivation of both RB1 and RBL2 restores transcriptional repression of *EZH2*, *SUZ12*, and *EED* promoters, which in turn brings about derepression of *CASP10*, *DAP1*, *HOXA5*, and *HRK* pro-apoptotic target genes and promotes lymphoma cell death. We have shown that the reason why RB1 becomes dephosphorylated is due primarily to decreased cyclin D1 expression, which depends on loss of TP53K372 methylation. Changes in methylation of TP53K372 probably affect its ability to interact with co-activator proteins and favors its association with co-repressors. In fact, our results support this notion because we have found that recruitment of TP53 to the *BCL3* promoter was unaffected, whereas binding of methylated TP53K372 was inhibited after PRMT5 inhibition. Concomitantly, binding of p300 to the *BCL3* promoter was reduced, and HDAC2 recruitment was increased. Previous work showed that the consequence of decreased BCL3 expression in H1299 or U2OS cells is formation and recruitment of NF-κB p52-HDAC1 repressor complexes to the cyclin D1 promoter (44). Our results support this model of cyclin D1 transcriptional repression as demonstrated by the gradual loss of BCL3 recruitment, persistent NF-κB p52 binding, and enrichment of HDAC1 at the cyclin D1 promoter in PRMT5 knockdown NHL cells.

One question that arises from these experiments is how PRMT5 inhibition triggers loss of TP53K372 methylation. It is known that TP53 is methylated at different sites by different lysine methyltransferases, including KMT7 and KMT3C (46, 48). In the same way that histones are demethylated by specific demethylases, TP53(Me_2)K370 is demethylated by KDM1 (LSD1), an event that renders TP53 less active (49). It is tempting to speculate that PRMT5 controls TP53K372 methylation by suppressing expression of a currently unidentified TP53K372 demethylase. Upon PRMT5 inhibition, derepression of this demethylase would reduce the levels of transcriptionally active, methylated TP53K372 and trigger *BCL3* repression. Another possibility is that PRMT5 may play an active role in the maintenance of KMT7 expression. In this case, PRMT5 knockdown would reduce KMT7 expression and *de novo* TP53K372 methylation. Currently, it is not clear if either or both scenarios are at work, but more investigation is required to determine the contribution of PRMT5 to post-translational regulation of TP53.

We have shown that PRMT5 knockdown results in cyclin D1 suppression and loss of RB1 phosphorylation in JeKo cells despite the fact that they lack TP53 expression. One interpretation of this result is that there are other mechanisms involved in regulating cyclin D1 expression, which are impacted by PRMT5 inhibition. In fact, cyclin D1 is known to be a direct target of the Wnt/β-catenin signaling pathway, which has recently been shown to be constitutively turned on in hepatocellular carcinoma cells through PRC2-mediated suppression of Wnt antagonists *AXIN2*, *NKD1*, *PPP2R2B*, *PRICKLE1*, and *SFRP5* (50). Therefore, it is possible that through its ability to promote PRC2 expression, PRMT5 indirectly contributes to Wnt antagonist suppression and that PRMT5 knockdown could inhibit Wnt/β-catenin signaling, thereby causing cyclin D1 transcriptional repression. Another possible explanation is that PRMT5 epigenetically silences cyclin D1-specific microRNAs, which become derepressed upon PRMT5 knockdown and inhibit cyclin D1 expression. Evidence in support of this mechanism of cyclin D1 regulation comes from recent findings that show that miR-33 inhibits cyclin D1 and CDK6 expression in Huh7 and A549 cell lines (30), and our results showing that, in addition to miR-33, PRMT5 epigenetically silences two other cyclin D1-specific microRNAs, miR-96 and miR-507, in JeKo cells.[3] Furthermore, ongoing studies in our

[3] V. Karkhanis and S. Sif, unpublished data.

laboratory have clearly shown that PRMT5 knockdown results in derepression of miR-33, miR-96, and miR-507.[3] It is worth noting that both transcriptional and translational regulatory mechanisms may be at play in JeKo cells as well as in other NHL cell lines, and it is going to be important to investigate to what extent each regulatory step influences cyclin D1 expression in the context of PRMT5 inhibition.

Our findings show that PRMT5 inhibition in mouse primary lymphoma cells results in reactivation of the RB1/RBL2-E2F tumor suppressor pathway; suppression of the PRC2 complex; and derepression of *DAP1*, *HOXA5*, and *HRK* pro-apoptotic genes. Furthermore, we have determined that the same regulatory networks restored in patient-derived NHL cell lines are also reactivated in Eμ-BRD2 primary lymphoma cells, as evidenced by loss of TP53K372 methylation and decreased expression of BCL3 and cyclin D1. Moreover, when we reduced PRMT5 expression in primary lymphoma cells and examined growth and survival *in vivo*, we discovered that transplant of *PRMT5*-specific shRNA-infected primary lymphoma cells into sublethally irradiated FVB mice resulted in significantly improved survival compared with the control group, establishing PRMT5 as an important molecular target and demonstrating that PRMT5 inhibition is a promising epigenetic therapy.

Acknowledgments—We thank A. N. Imbalzano for providing lentiviral expression vectors and H. Al Omrani for help with mouse normal B cell and primary lymphoma cell purification.

REFERENCES

1. Küppers, R., Klein, U., Hansmann, M. L., and Rajewsky, K. (1999) Cellular origin of human B-cell lymphoma. *N. Engl. J. Med.* **341,** 1520–1529
2. Stevenson, F. K., Sahota, S. S., Ottensmeier, C. H., Zhu, D., Forconi, F., and Hamblin, T. J. (2001) The occurrence and significance of V gene mutations in B cell-derived human malignancy. *Adv. Cancer Res.* **83,** 81–116
3. Nogai, H., Dörken, B., and Lenz, G. (2011) Pathogenesis of non-Hodgkin's lymphoma. *J. Clin. Oncol.* **29,** 1803–1811
4. Swerdlow, S. H., Campo, E., Seto, M., and Müller-Hemrelink, H. K. (2008) Mantle cell lymphoma. in *WHO Classification of Tumours of Haematopoietic and Lymphoid Tissues* (Swerdlow, S. H., Campo, E., Harris, N. L., Jaffe, E. S., Pileri, S. A., Stein, H., Thiele, J., and Vardiman, J. W. eds) pp. 229–232, IARC Publishing Group, Lyon, France
5. Fisher, R. I., Dahlberg, S., and Nathwani, B. (1995) A clinical analysis of two indolent lymphoma entities: mantle cell lymphoma and marginal zone lymphoma (including the mucosa-associated lymphoid tissue and monocytoid B-cell subcategories): a Southwest Oncology Group study. *Blood* **85,** 1075–1082
6. Teodorovic, I., Pittaluga, S., and Kluin-Nelemans, J. C. (1995) Efficacy of four different regimens in 64 mantle-cell lymphoma cases: clinicopathologic comparison with 498 other non-Hodgkin's lymphoma subtypes–European Organization for the Research and Treatment of Cancer Lymphoma Cooperative Group. *J. Clin Oncol.* **13,** 2819–2826
7. Alizadeh, A. A., Eisen, M. B., Davis, R. E., Ma, C., Lossos, I. S., Rosenwald, A., Boldrick, J. C., Sabet, H., Tran, T., Yu, X., Powell, J. I., Yang, L., Marti, G. E., Moore, T., Hudson, J., Jr., Lu, L., Lewis, D. B., Tibshirani, R., Sherlock, G., Chan, W. C., Greiner, T. C., Weisenburger, D. D., Armitage, J. O., Warnke, R., Levy, R., Wilson, W., Grever, M. R., Byrd, J. C., Botstein, D., Brown, P. O., and Staudt, L. M. (2000) Distinct types of diffuse large B-cell lymphoma identified by gene expression profiling. *Nature* **403,** 503–511
8. Rosenwald, A., Wright, G., Chan, W. C., Connors, J. M., Campo, E., Fisher, R. I., Gascoyne, R. D., Muller-Hermelink, H. K., Smeland, E. B., Giltnane, J. M., Hurt, E. M., Zhao, H., Averett, L., Yang, L., Wilson, W. H., Jaffe, E. S., Simon, R., Klausner, R. D., Powell, J., Duffey, P. L., Longo, D. L., Greiner, T. C., Weisenburger, D. D., Sanger, W. G., Dave, B. J., Lynch, J. C., Vose, J., Armitage, J. O., Montserrat, E., López-Guillermo, A., Grogan, T. M., Miller, T. P., LeBlanc, M., Ott, G., Kvaloy, S., Delabie, J., Holte, H., Krajci, P., Stokke, T., and Staudt, L. M. (2002) The use of molecular profiling to predict survival after chemotherapy for diffuse large-B-cell lymphoma. *N. Engl. J. Med.* **346,** 1937–1947
9. Hanahan, D., and Weinberg, R. (2011) Hallmarks of cancer: the next generation. *Cell* **144,** 646–674
10. Baylin, S. B., and Jones, P. A. (2011) A decade of exploring the cancer epigenome–biological and translational implications. *Nat. Rev. Cancer* **11,** 726–734
11. Bracken, A. P., and Helin, K. (2009) Polycomb group proteins: navigators of lineage pathways led astray in cancer. *Nat. Rev. Cancer* **9,** 773–784
12. Chi, P., Allis, C. D., and Wang, G. G. (2010) Covalent histone modifications–miswritten, misinterpreted and mis-erased in human cancers. *Nat. Rev. Cancer* **10,** 457–469
13. Füllgrabe, J., Kavanagh, E., and Joseph, B. (2011) Histone onco-modifications. *Oncogene* **30,** 3391–3403
14. Karkhanis, V., Hu, Y. J., Baiocchi, R. A., Imbalzano, A. N., and Sif, S. (2011) Versatility of PRMT5-induced methylation in growth control and development. *Trends Biochem. Sci.* **36,** 633–641
15. Yang, Y., and Bedford, M. T. (2013) Protein arginine methyltransferases and cancer. *Nat. Rev. Cancer* **13,** 37–50
16. Chase, A., and Cross, N. C. (2011) Aberrations of EZH2 in cancer. *Clin. Cancer Res.* **17,** 2613–2618
17. Pal, S., Baiocchi, R. A., Byrd, J. C., Grever, M. R., Jacob, S. T., and Sif, S. (2007) Low levels of miR-92b/96 induce PRMT5 translation and H3R8/H4R3 methylation in mantle cell lymphoma. *EMBO J.* **26,** 3558–3569
18. Wang, L., Pal, S., and Sif, S. (2008) Protein arginine methyltransferase 5 suppresses the transcription of the RB family of tumor suppressors in leukemia and lymphoma cells. *Mol. Cell. Biol.* **28,** 6262–6277
19. Tae, S., Karkhanis, V., Velasco, K., Yaneva, M., Erdjument-Bromage, H., Tempst, P., and Sif, S. (2011) Bromodomain protein 7 interacts with PRMT5 and PRC2, and is involved in transcriptional repression of their target genes. *Nucleic Acids Res.* **39,** 5424–5438
20. Simon, J. A., and Kingston, R. E. (2009) Mechanisms of Polycomb gene silencing: knowns and unknowns. *Nat. Rev. Mol. Cell Biol.* **10,** 697–708
21. Margueron, R., and Reinberg, D. (2011) The Polycomb complex PRC2 and its mark in life. *Nature* **469,** 343–349
22. Harbour, J. W., and Dean, D. C. (2000) The Rb/E2F pathway: expanding roles and emerging paradigms. *Genes Dev.* **14,** 2393–2409
23. Bracken, A. P., Pasini, D., Capra, M., Prosperini, E., Colli, E., and Helin, K. (2003) Margueron. *EMBO J.* **22,** 5323–5335
24. Karkhanis, V., Wang, L., Tae, S., Hu, Y. J., Imbalzano, A. N., and Sif, S. (2012) Protein arginine methyltransferase 7 regulates cellular response to DNA damage by methylating promoter histones H2A and H4 of the polymerase δ catalytic subunit gene, *POLD1*. *J. Biol. Chem.* **287,** 29801–29814
25. Campeau, E., Ruhl, V. E., Rodier, F., Smith, C. L., Rahmberg, B. L., Fuss, J. O., Campisi, J., Yaswen, P., Cooper, P. K., and Kaufman, P. D. (2009) A versatile viral system for expression and depletion of proteins in mammalian cells. *PLoS ONE* **4,** e6529
26. Greenwald, R. J., Tumang, J. R., Sinha, A., Currier, N., Cardiff, R. D., Rothstein, T. L., Faller, D. V., and Denis, G. V. (2004) Eμ-*BRD2* transgenic mice develop B-cell lymphoma and leukemia. *Blood* **103,** 1475–1484
27. Wang, L., Baiocchi, R. A., Pal, S., Mosialos, G., Caligiuri, M., and Sif, S. (2005) The BRG1- and hBRM-associated factor BAF57 induces apoptosis by stimulating expression of the cylindromatosis tumor suppressor gene. *Mol. Cell. Biol.* **25,** 7953–7965
28. Pal, S., Vishwanath, S. N., Erdjument-Bromage, H., Tempst, P., and Sif, S. (2004) Human SWI/SNF-associated PRMT5 methylates histone H3 arginine 8 and negatively regulates expression of *ST7* and *NM23* tumor suppressor genes. *Mol. Cell. Biol.* **24,** 9630–9645
29. Agostinelli, C., Paterson, J. C., Gupta, R., Righi, S., Sandri, F., Piccaluga, P. P., Bacci, F., Sabattini, E., Pileri, S. A., and Marafioti T. (2012) Detection of LIM domain only 2 (LMO2) in normal human tissues and haematopoietic and non-haematopoietic tumours using a newly developed rabbit monoclonal antibody. *Histopathology* **61,** 33–46

30. Cirera-Salinas, D., Pauta, M., Allen, R. M., Salerno, A. G., Ramírez, C. M., Chamorro-Jorganes, A., Wanschel, A. C., Lasuncion, M. A., Morales-Ruiz, M., Suarez, Y., Baldan, Á., Esplugues, E., and Fernández-Hernando, C. (2012) Mir-33 regulates cell proliferation and cell cycle progression. *Cell Cycle* **11,** 922–933
31. Hans, C. P., Weisenburger, D. D., Greiner, T. C., Gascoyne, R. D., Delabie, J., Ott, G., Müller-Hermelink, H. K., Campo, E., Braziel, R. M., Jaffe, E. S., Pan, Z., Farinha, P., Smith, L. M., Falini, B., Banham, A. H., Rosenwald, A., Staudt, L. M., Connors, J. M., Armitage, J. O., and Chan, W. C. (2004) Confirmation of the molecular classification of diffuse large B-cell lymphoma by immunohistochemistry using a tissue microarray. *Blood* **103,** 275–282
32. Pietersen, A. M., Horlings, H. M., Hauptmann, M., Langerød, A., Ajouaou, A., Cornelissen-Steijger, P., Wessels, L. F., Jonkers, J., van de Vijver, M. J., and van Lohuizen, M. (2008) EZH2 and BMI1 inversely correlate with prognosis and TP53 mutation in breast cancer. *Breast Cancer Res.* **10,** R109
33. Varambally, S., Dhanasekaran, S. M., Zhou, M., Barrette, T. R., Kumar-Sinha, C., Sanda, M. G., Ghosh, D., Pienta, K. J., Sewalt, R. G., Otte, A. P., Rubin, M. A., and Chinnaiyan, A. M. (2002) The polycomb group protein EZH2 is involved in progression of prostate cancer. *Nature* **419,** 624–629
34. Visser, H. P., Gunster, M. J., Kluin-Nelemans, H. C., Manders, E. M., Raaphorst, F. M., Meijer, C. J., Willemze, R., and Otte, A. P. (2001) The Polycomb group protein EZH2 is upregulated in proliferating, cultured human mantle cell lymphoma. *Br. J. Haematol.* **112,** 950–958
35. Kirmizis, A., Bartley, S. M., Kuzmichev, A., Margueron, R., Reinberg, D., Green, R., and Farnham, P. J. (2004) Silencing of human polycomb target genes is associated with methylation of histone H3 Lys 27. *Genes Dev.* **18,** 1592–1605
36. Bracken, A. P., Dietrich, N., Pasini, D., Hansen, K. H., and Helin, K. (2006) Genome-wide mapping of Polycomb target genes unravels their roles in cell fate transitions. *Genes Dev.* **20,** 1123–1136
37. Wang, J., Chun, H. J., Wong, W., Spencer, D. M., and Lenardo, M. J. (2001) Caspase-10 is an initiator caspase in death receptor signaling. *Proc. Natl. Acad. Sci. U.S.A.* **98,** 13884–13888
38. Deiss, L. P., Feinstein, E., Berissi, H., Cohen, O., and Kimchi, A. (1995) Identification of a novel serine/threonine kinase and a novel 15-kD protein as potential mediators of the γ interferon-induced cell death. *Gene Dev.* **9,** 15–30
39. Chen, H., Chung, S., and Sukumar, S. (2004) HOXA5-induced apoptosis in breast cancer cells in mediated by caspases 2 and 8. *Mol. Cell. Biol.* **24,** 924–935
40. Inohara, N., Ding, L., Chen, S., and Núñez, G. (1997) *harakiri*, a novel regulator of cell death, encodes a protein that activates apoptosis and interacts selectively with survival-promoting proteins Bcl-2 and Bcl-X_L. *EMBO J.* **16,** 1686–1694
41. Schug, J. (2008) Using TESS to predict transcription factor binding sites in the DNA sequence. *Curr. Protoc. Bioinformatics* 21:2.6.1–2.6.15 10.1002/0471250953.bi0206s21
42. Giacinti, C., and Giordano, A. (2006) RB and cell cycle progression. *Oncogene* **25,** 5220–5227
43. Kim, J. K., and Diehl, J. A. (2009) Nuclear cyclin D1: an oncogenic driver in human cancer. *J. Cell. Physiol.* **220,** 292–296
44. Rocha, S., Martin, A. M., Meek, D. W., and Perkins, N. D. (2003) p53 represses cyclin D1 transcription through down regulation of Bcl-3 and inducing association of the p52 NF-κB subunit with histone deacetylase 1. *Mol. Cell. Biol.* **23,** 4713–4727
45. Amin, H. M., McDonnell, T. J., Medeiros, L. J., Rassidakis, G. Z., Leventaki, V., O'Connor, S. L., Keating, M. J., and Lai, R. (2003) Characterization of 4 mantle cell lymphoma cell lines. *Arch. Pathol. Lab. Med.* **127,** 424–431
46. Chuikov, S., Kurash, J. K., Wilson, J. R., Xiao, B., Justin, N., Ivanov, G. S., McKinney, K., Tempst, P., Prives, C., Gamblin, S. J., Barlev, N. A., and Reinberg, D. (2004) Regulation of p53 activity through lysine methylation. *Nature* **432,** 353–360
47. Lenburg, M. E., Sinha, A., Faller, D. V., and Denis, G. V. (2007) Tumor-specific and proliferation-specific gene expression typifies murine transgenic B cell lymphomagenesis. *J. Biol. Chem.* **282,** 4803–4811
48. Huang, J., Perez-Burgos, L., Placek, B. J., Sengupta, R., Richter, M., Dorsey, J. A., Kubicek, S., Opravil, S., Jenuwein, T., and Berger, S. L. (2006) Repression of p53 activity by Smyd2-mediated methylation. *Nature* **444,** 629–632
49. Huang, J., Sengupta, R., Espejo, A. B., Lee, M. G., Dorsey, J. A., Richter, M., Opravil, S., Shiekhattar, R., Bedford, M. T., Jenuwein, T., and Berger, S. L. (2007) p53 is regulated by the lysine demethylase LSD1. *Nature* **449,** 105–108
50. Cheng, A. S., Lau, S. S., Chen, Y., Kondo, Y., Li, M. S., Feng, H., Ching, A. K., Cheung, K. F., Wong, H. K., Tong, J. H., Jin, H., Choy, K. W., Yu, J., To, K. F., Wong, N., Huang, T. H., and Sung, J. J. (2011) EZH2-mediated concordant repression of Wnt antagonists promotes β-catenin-dependent hepatocarcinogenesis. *Cancer Res.* **71,** 4028–4039